



Article

The Residue Chemistry Transformation Linked to the Fungi Keystone Taxa during Different Residue Tissues Incorporation into Mollisols in Northeast China

Qilin Zhang ^{1,2}, Xiujun Li ^{1,2}, Guoshuang Chen ¹ , Nana Luo ¹, Jing Sun ^{1,2}, Ezemaduka Anastasia Ngozi ³  and Xinrui Lu ^{1,*}

¹ State Key Laboratory of Black Soils Conservation and Utilization, Northeast Institute of Geography and Agroecology, Chinese Academy of Sciences, Changchun 130102, China; zhangqilin@iga.ac.cn (Q.Z.); lixiujun@iga.ac.cn (X.L.); chenguoshuang@iga.ac.cn (G.C.); luonana@iga.ac.cn (N.L.); sunjing@iga.ac.cn (J.S.)
² University of Chinese Academy of Sciences, Beijing 100049, China
³ School of Life Science, Peking University, Beijing 100091, China; anasha0707@tom.com
* Correspondence: luxinrui@iga.ac.cn

Abstract: Managing carbon input from crop straw in cropland ecosystems could increase soil organic carbon (SOC) sequestration to achieve C neutrality and mitigate climate change. The complexity of the chemical structures of crop residue largely affects SOC sequestration. Fungi communities play an important role in the degradation of crop residues. However, the relationship between the fungal community composition and the chemical structures of crop residues remains unclear and requires further investigation. Therefore, a 120-day incubation experiment was conducted in Mollisols in Northeast China to investigate the decomposition processes and dynamics of maize straw stem (ST), leaf (LE) and sheath (SH) residues using ¹³C-NMR spectroscopy. Additionally, the microbiomes associated with these residues were analyzed through high-throughput sequencing to explore their relationship. Our results showed that the alkyl C contents in all treatments exhibited increases ranging from 15.1% to 49.1%, while the O-alkyl C contents decreased, ranging from 0.02% to 11.2%, with the incubation time. The A/OA ratios of ST, LE and SH treatments were increased by 23.7%, 43.4% and 49.3% with incubation time, respectively. During the early stages of straw decomposition, Ascomycota dominated, and in the later stage, Basidiomycota were predominant. The class of *Sordariomycetes* played a key role in the chemistry transformation of straw tissues during decomposition. The keystone taxa abundances, *Fusarium_kyushuense*, and *Striatibotrys_eucylindrospora*, showed strong negative correlations with di-O-alkyl C and carbonyl-C content and positive correlations with the β-glucosidase and peroxidase enzyme activity, respectively. In conclusion, our study demonstrated that the keystone taxa play a significant role in regulating the chemical structures of straw tissues, providing a better understanding of the influence of residue quality on SOC sequestration.

Keywords: ¹³C-NMR spectroscopy; chemical structure; straw tissues; fungi keystone taxa; extracellular enzyme activity



Citation: Zhang, Q.; Li, X.; Chen, G.; Luo, N.; Sun, J.; Ngozi, E.A.; Lu, X. The Residue Chemistry Transformation Linked to the Fungi Keystone Taxa during Different Residue Tissues Incorporation into Mollisols in Northeast China. *Agriculture* **2024**, *14*, 792. <https://doi.org/10.3390/agriculture14060792>

Academic Editor: Fernando P. Carvalho

Received: 11 April 2024

Revised: 6 May 2024

Accepted: 15 May 2024

Published: 21 May 2024



Copyright: © 2024 by the authors. Licensee MDPI, Basel, Switzerland. This article is an open access article distributed under the terms and conditions of the Creative Commons Attribution (CC BY) license (<https://creativecommons.org/licenses/by/4.0/>).

1. Introduction

More than 10% of global soil organic carbon (SOC) is stored in cropland ecosystems [1]. The substantial SOC storage in croplands can be attributed to the large-scale implementation of crop straw return policies since 2000 [2]. Crop straw decomposition plays a crucial role in C and nutrient cycling and mitigates climate change [3]. Bacteria and fungi are the major domains responsible for approximately 90% of all organic matter decomposition processes [4]. However, most studies have focused on litter decomposition in forests [5–7]; less attention has been paid to this ecological process in agricultural lands.

Crop residue decomposition is a microbial-driven process induced and characterized by mass loss [8]. It is influenced by biotic and abiotic factors [9,10]. Abiotic factors, such as

soil moisture, temperature [11], climate [10], soil fertility and soil types [12] and placement depths and locations [9], indirectly influence the rate of straw decomposition. Additionally, straw quality emerges as a crucial predictor of residue decomposition [13]. For example, *Astragalus mongholicus* exhibited the highest residue decomposition rate in field experiments, while *Festuca ovina* showed the slowest rate [14]. And Pascault et al. (2010) found that the alfalfa decomposed faster than wheat straw in an 11-month field experiment [15]. In addition, several studies investigated how the different tissues of straw affected its decomposition process [14,16]. For example, one study revealed that crop leaf residues decomposed more rapidly compared to stems and roots [17]. Another study suggested that shoot residues had a higher decomposition rate than root residues, particularly in the first 12 days [13]. Moreover, the chemical structure of crop straw was also a significant factor affecting the decomposition of the residues [18]. Studies have shown a positive relationship between the proportions of decomposed C among different residues and the mass losses of O-alkyl C, di-O-alkyl C and carbonyl C [1]. However, no consensus has been reached regarding the alterations in carbon functional groups within the chemical structure of straw residues during decomposition. For example, Li et al. (2020a) observed decreases in di-O-alkyl and O-alkyl C contents, while noting increases in alkyl and N-alkyl/methoxyl C contents, during the initial 4 months of wheat straw degradation [2]. Similarly, Wang et al. (2012a) reported a decrease in carbohydrate abundance and increases in aromatics and aliphatics during plant residue decomposition. Furthermore, another study found that O/N-alkyl carbons decreased, while aromatic carbons, aromatic C–O groups, and COO/N–C=O groups increased during maize and wheat straw decomposition processes [10]. Therefore, it is necessary to explore the changes in carbon's chemical structure during the degradation of different straw tissues.

Microbial communities were an important driver during residue decomposition, known as the 'Decomposer Control Hypothesis' [19]. This indicated that the types of decomposer communities exerted predominant control over the chemical changes in the decomposing residues [20]. Moreover, the fungi exhibited greater efficiency in attacking the recalcitrant lignocellulose matrix compared to other organisms due to their ability to produce a diverse array of extracellular enzymes [21,22]. The contribution of fungi to the degradation of residues at different stages of degradation remains controversial. For example, studies have shown that fungi only dominate the later stages of degradation [23], while other studies have reported that fungi played an important role throughout all stages of residue decomposition [24]. Within fungi communities, Ascomycota prevail during the early stages of decomposition and are replaced by Basidiomycota later on [25]. Numerous studies have proved that the major two phyla, Ascomycota and Basidiomycota, exhibit a preference for decomposing plant materials [26–28]. Meanwhile, the decomposed residues themselves could also affect the composition and functioning of the microbial community based on the chemical structure [29]. For example, Baumann et al. (2009) found that the microbial community composition depended on the aryl C contents of wheat and vetch straws and the O-alkyl C content of eucalypt straw at the end of decomposition [30]. More specifically, Li et al. (2020) observed decreases in di-O-alkyl and O-alkyl C, along with increases in alkyl, aryl and carboxyl/amide C contents, during wheat and maize straw decomposition, which were associated with a decline [2]. Additionally, the aromatic C-H exhibited negative correlation with the *Pseudogymnoascus roseus* sp. (belonging to Ascomycota phylum), while CH/CH₂ abundances showed positive correlation [20]. This finding aligns with the studies of Liu et al. (2016) and Bonanomi et al. (2019), who described close relationships between the temporal dynamics of litter chemistry and decomposer composition over 7-month and 180-day periods, respectively [5,31]. However, few studies have investigated how changes in carbon functional groups during different straw tissue degradation processes are associated with fungal community succession.

The activities of extracellular enzymes produced by fungi have received considerable attention due to their contribution to the processes controlling decomposition [22,32]. Among the soil hydrolytic enzymes frequently measured, β -glucosidase (β GC) is used to

acquire C by hydrolyzing cellulose [33], and β -xylosidase (β X) dominates the decomposition of polysaccharides [34]. Two oxidative enzymes, phenol oxidase and peroxidase, could depolymerize lignin by consuming oxygen and oxidized phenol and using H_2O_2 as an acceptor, respectively [35]. Moreover, residues with different chemical qualities may require varying amounts of enzymes during decomposition, as the labile substances are easily degraded by microorganisms via the secretion of hydrolases during the early stages of decomposition [36], while macromolecular compounds, such as lignin and phenol, can be utilized by microdecomposers that secrete oxidase during the later stages of decomposition [37]. Notably, the responses of extracellular enzymes activities vary depending on the residues' chemical structures during decomposition. For example, increases in oxidative enzymes were positively associated with the litter with higher alkyl/O-alkyl C ratios while negatively associated with O-alkyl C [38]. However, the relationship among fungal community succession, exogenous enzyme activity and carbon functional group changes within straw tissue during different degradation processes is still unclear.

The process of residue decomposition involves a substantial number of microbes, and their interactions play a crucial role in determining the outcome of decomposition. Recent studies have found that the abundance and diversity of microbes could not fully explain the functions of the entire microbial community [39,40]. Further, network analysis could uncover complex relationship within microbial communities and provide insights beyond abundance and diversity. The keystone taxa identified through network analysis are highly connected and exert significant influence on both the structures and functions of microbial communities [41,42]. For instance, straw decomposition had strong positive associations with the relative abundance of bacterial, as well as fungal keystone taxa [41]. In general, fungi could degrade recalcitrant carbon sources by secreting extracellular enzymes such as *Penicillium* and *Aspergillus*, which show high efficiency in degrading crop-based materials [43]. A pertinent question arises regarding whether these keystone taxa play a role in secreting extracellular enzymes to degrade crop residues. Therefore, it is imperative to investigate the relationships between the keystone taxa of fungi, extracellular enzyme activities and chemical structures of straw tissue.

Therefore, we conducted an incubation experiment for 120 days to investigate the temporal succession of the chemical structures of straw tissues and the regulatory roles of keystone taxa in this process through their influence on extracellular enzyme production and fungal community composition. The objectives of this study were (i) to investigate how changes in carbon functional groups during different straw tissue degradation processes were associated with fungal community succession, (ii) to identify keystone taxa by constructing co-occurrence networks based on high-throughput sequencing, and (iii) to further explore the inter-relationship between residue decomposition, fungi keystone taxa and extracellular enzyme function via structural equation modeling (SEM).

2. Materials and Methods

2.1. Experimental Site and Soil Characteristics

The Mollisols utilized in the present study originated from permanent maize (*Zea mays* L.) cultivation in the field at the Northeast Institute of Geography and Agroecology, the Chinese Academy of Sciences, Jilin Province (43°59'51" N, 125°24'5" E). The location in question has a monsoon climate that is characteristic of the middle latitudes, with an average temperature for the year of 4.4 °C and an average precipitation rate of 520 mm. Mollisol soil of this kind was discovered in the field [44].

Prior to the experiment, maize was put in cultivation in May 2022, and samples of the soil were taken from the plowing layer (0–20 cm) of the field. Subsequently, after being frozen, soil samples were taken to the laboratory in various containers. The samples were then homogenized and subsequently passed through a 2 mm sieve after all visible stone blocks and residues had been removed with tweezers. Before participating in an incubation experiment, the samples were kept in storage for no longer than two weeks at 4 °C. Subsamples of the soil were air-dried in order to examine its physicochemical

properties. Table S1 illustrates the fundamental properties of the soil (0–20 cm) that were utilized in this experiment.

2.2. Incubation Experimental Design

There were four independent treatments, six intervals, three separate rounds of destructive sampling, and 72 groups in this experiment. Soil and straw samples were taken for examination, and each treatment was run through three replications. In each of the four treatments, one of the following forms of ^{13}C -labeled straw was added to the soil: (1) the stem (ST), (2) the leaf (LE), (3) the sheath (SH) or (4) soil without any straw addition (CK). The detailed characteristics of this incubation experiment are described in the article in [45].

Prior the experiment beginning, 100 g of soil taken from maize farming fields was loaded into 500 mL wide-mouthed bottles. The bottles holding the soil samples were incubated beforehand in a dark room at a temperature of 25 degrees for an entire week after having been adjusted to 45% WHC with sterile deionized water. After that, segments of the ^{13}C -labeled corn stems, leaves or sheaths were added into those containers and thoroughly mixed with the soil. The water content of the soil was modified to 65% WHC to ensure optimum microbial growth. The incubation conditions in the CK group were identical to those in the other three treatment groups containing soil with additional maize straw tissues. The entire study was carried out for a period of 120 days in darkness at 25 °C. A 5 g subsample of soil coming from every replicate was collected on the sampling days for microbial community composition analysis. Some of the samples were stored at –80 °C. The remaining soil samples were dried to measure the physicochemical properties of the soil. The four treatments that had three replicates were destructive sampling at 5, 10, 20, 40, 80 and 120 days. A total of 12 groups were selected each time.

2.3. Amplification and Sequencing of Fungal ITS RNA

The ITS region of the fungal rRNA gene was amplified via PCR (95 °C for 5 min, followed by 30 cycles at 95 °C for 45 s, 50 °C for 50 s and 75 °C for 40 s and a final extension at 72 °C for 10 min) using the primers SSU0817F (5'-barcode-CTTGGTCATTTAGAGGAAGTAA-3') and SSU1196R (5'-GCTGCGTTCTTCATCGATGC-3'), where the barcode is a unique eight-base sequence for each sample. The PCR products were detected via electrophoresis in 2% agarose gel, and the samples were mixed in equal quantities according to the concentration of PCR products. After being fully mixed, the samples were detected again via electrophoresis in 2% agarose gel. The target bands were recovered using a gel recovery kit provided by Qiagen. A NEBNext® Ultra™ IIDNA Library Prep Kit (Illumina San Diego, CA, USA) was used to construct the library, and the constructed library was subjected to Qubit and Q-PCR quantification. After the libraries were qualified, NovaSeq6000 (Illumina, San Diego, CA, USA) was used for sequencing. Purified amplicons were pooled in equimolar and paired-end sequenced (2 × 250) via an Illumina MiSeq platform according to the standard protocols.

2.4. ^{13}C Nuclear Magnetic Resonance (NMR) Spectroscopy

The chemical composition of soil C was characterized using solid-state magic-angle spinning (MAS) nuclear magnetic resonance (NMR). A Bruker Avance III 400 spectrometer (Bruker BioSpin, Rheinstetten, Germany) with a resonance frequency of 100.62 MHz for ^{13}C was used to spin the soil samples five times after they had been treated with 50 mL of 10% HF, 50 mL of 10% HCl and distilled water. The samples were then dried, pressed and placed onto 7-millimeter zirconia rotors. Applying cross polarization with total suppression of spinning sidebands (TOSS) pulse program, which consisted of a ramp-contact, 0.5 s relaxation delay, ramp-contact and small-phase incremental alternation with 64 steps (SPINAL64) decoupling pulse program, improved the signal-to-noise ratio. The methane C atoms of adamantane served as an external standard for calibrating the spectra, which were recorded as the total of 15,000 scans ($\delta = 29.47$ ppm). The chemical shift limits' spectra were used to estimate the general C types. The ratios between the relative intensities of the

0–45 and 45–110 ppm regions (alkyl C/O-alkyl C), as well as the 110–160 and 45–110 ppm regions (aryl C/O-alkyl C), were used as indicators of decomposition [46].

2.5. Extracellular Enzyme Activity (EEA) Assays

Two hydrolytic enzymes (β -1,4-glucosidase (β GC), β -1,4-xylosidase (β X) and two oxidative enzymes (phenol oxidase (PPO) and peroxidase (POD)) were analyzed after straw tissues were decomposed for 10 d, 20 d, 40 d, 80 d and 120 d. The analysis of the four hydrolytic enzymes was performed using 96-well microplates according to the method previously described [47].

2.6. Statistical Analyses

The significance levels ($p < 0.05$) of the relative contents (%) of soil C chemical form structure, abundances of fungal phyla abundance, extracellular enzyme activity and fungi community diversity indexes using SPSS, ver. 22.0 (SPSS Inc., Chicago, IL, USA) were determined via one-way analysis of variance (ANOVA). To evaluate the organization of fungal communities, weighted UniFrac distances were the basis for principal coordinate analysis (PCoA). Network analysis was utilized to assess the complexity of the microbiome and pinpoint the possible keystone taxa in the soil treatment groups. We only examined fungal OTUs with relative abundances greater than 0.005%. We computed correlation networks using the R igraph tool. Using pair relations with a coefficient > 0.7 ($p < 0.05$, two-sided), the co-occurrence network was constructed. SparCC analysis was used to find OTU correlations. Using the Fruchterman–Reingold arrangement, the network topology was investigated and visualized using the interactive Gephi (v.0.10.1) platform. Value importance in projection (VIP) via partial least squares (PLS) regression was used as a predictor to estimate the importance of the OTUs encountered in the network relative to EEA in order to determine the keystone taxa of the co-occurrence network. The EEA content predictors were found by fitting the PLS regression. High-throughput omics data partial least squares were computed using the R package mixOmics. Value importance in projection (VIP) was used to rank the predictors. Greater VIP values in PLS regression signify an increased contribution. Relevant predictors were identified as those with a $VIP > 1$. The keystone species were then identified as the OTUs with high degrees in the network (the top 5 inside each dominating module) and high VIP values ($VIP > 1$). Redundancy analysis (RDA) was applied to investigate the relationships among the chemical structures of straw tissues, extracellular enzymes and fungi keystone taxa abundance for different treatments. Multivariate regression tree (MRT) analysis was also used to explore the interactions between C chemical forms and fungi communities. The statistical analyses were undertaken in R (v4.0.2; <http://www.r-project.org/>; accessed on 11 April 2024).

3. Results

3.1. The Decomposition of Straw Tissues

Figure 1 shows that the proportions of ST, LE and SH decomposition, which is indicated by the change in carbon content. One-way ANOVA analysis revealed that the proportion of straw decomposition was affected by both the stage and tissue types (Table S1). The proportions of ST, LE and SH decomposition during the incubation stage ranged from 7.6% to 58.4%, 13.7% to 62.4% and 10.8% to 35.6%, respectively. At the end of incubation, the decomposition proportions for treatments were in the order of $LE > ST > SH$ ($p < 0.05$). The dynamics of the decomposition proportions among three treatments exhibited similar patterns characterized by a rapid decomposition stage and a slow decomposition stage.

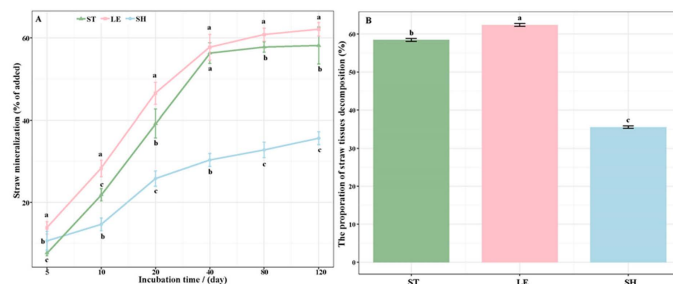


Figure 1. The proportions of straw tissue stem (ST), leaf (LE) and sheath (SH) decomposition represented by the carbon (C) content remaining. The changes in the C content remaining with the decomposition time in (A). The total proportions of straw tissue decomposition at days 120 of incubation in (B). Lowercase letters represent significant differences between ST, LE and SH ($p < 0.05$).

3.2. ¹³C Nuclear Magnetic Resonance (NMR) Spectroscopy

The ¹³C-NMR spectra of ST, LE and SH treatments at incubation days 80 and 120 are shown in Figure 2. The comprehensive spectra exhibit signals from all C functional groups categorized to four chemical shift regions: alkyl C (0–45 ppm), O-alkyl C (45–110 ppm), aromatic C (110–160 ppm) and carbonyl C (160–220 ppm).

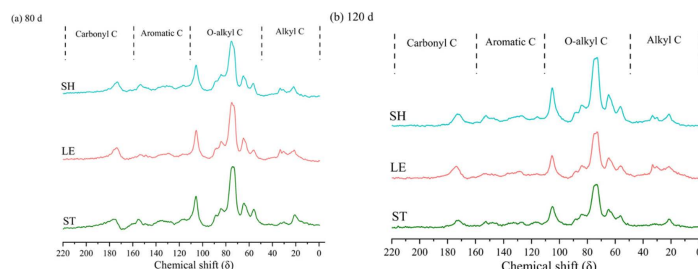


Figure 2. Exemplary spectra of straw tissue stems (ST), leaves (LE) and sheaths (SH) sampled on incubation days 80 and 120.

Tables 1 and 2 reveals the changes in C functional groups during ST, LE and SH decomposition. Across all treatments, O-alkyl C dominated the ¹³C-NMR spectra with a relative abundance of 58.9–69.9%. The proportion of Alkyl C increased by 15.1–49.1%, while the proportion of O-alkyl C decreased by 0.02–11.2% over time. At 80 d, the O-alkyl C proportions of LE were 6.2% and 7.7% greater than those of ST and SH, respectively. The alkyl C proportions of ST and LE were greater than that of SH at both 80 d and 120 d. The A/OA ratio for each treatment followed the order of ST > LE > SH at 80 d, while it changed to LE > ST > SH at 120 d. With incubation time, the A/OA ratio increased by 23.7%, 43.4% and 49.3% for the ST, LE and SH treatments, respectively. These results indicated that the stem, leaf and sheath tissues undergo degradation with the incubation time, with leaves being the most degraded.

Table 1. Percentage contribution of C functional groups based on the integration of the ¹³C-NMR spectra of straw stems, leaves and sheaths.

		O-Alkyl C (45–110 ppm)			Aromatic C (110–160 ppm)			Carbonyl C (160–220 ppm)	A/OA	AL/AR
		Alkyl C (0–45 ppm)	O/N-alkyl C	di-O-alkyl C	Total	Aryl C/O-aryl C	Phenolic C			
80d	ST	11.59	55.26	10.30	65.56	7.75	6.18	13.93	0.18	3.38
	LE	10.17	57.49	12.40	69.89	2.68	4.96	7.64	0.15	4.02
	SH	5.42	50.05	14.43	64.48	10.31	7.55	17.86	0.08	2.32
120d	ST	13.66	47.58	11.36	58.94	11.69	3.98	15.68	0.23	2.65
	LE	16.25	52.01	11.17	63.18	6.66	3.16	9.83	0.26	3.86
	SH	10.68	50.05	14.42	64.47	6.70	7.38	17.48	0.16	3.02

Note: ST implies the stems tissues of maize straw LE implies the leaf tissues of maize straw; SH implies the sheath tissues of maize straw.

Table 2. C-types found in important biomolecules (based on [48]) and percentage of C assigned to those biomolecules in stem, leaves and sheath residues.

Biomolecule	C-Type	80d			120d		
		ST	LE	SH	ST	LE	SH
Carbohydrate	O-alkyl, di-O-alkyl	65.56	69.89	64.48	58.94	63.18	64.47
Protein	alkyl, N-alkyl, carbonyl	20.51	22.47	17.66	25.38	26.99	18.06
Lignin	alkyl, N-alkyl, O-alkyl, aryl, O-aryl	80.78	75.30	73.33	76.92	78.09	78.20
Lipid	alkyl	11.59	10.17	5.42	13.66	16.25	10.68

3.3. Soil Community Composition and the Co-Occurrence Network of Fungi

The characteristics of the fungi communities of the ST, LE, SH and CK groups are illustrated in Figure 3. PCoA analysis based on weighted UniFrac revealed distinct differences in the fungi community's structure across all the treatments (Figure 3A). PC1 and PC2 accounted for 52.98% and 19.08% of variations in fungi communities, respectively. Straw tissue application significantly altered fungi diversity ($p < 0.05$, Figure 3C,D). The OTU abundance decreased by 33.3%, 12.0%, 10.0% and 14.2% for ST, LE, SH and CK treatments following incubation, respectively ($p < 0.05$), while the Simpson index increased by 11.3%, 5.6% and 3.3%, respectively ($p < 0.05$). The OTU abundance of CK was 7.2–17.6% greater compared to those of the ST, LE and SH treatments, while the Simpson index was 7.0–10.1% lower ($p < 0.05$). This finding suggested that a subgroup of the soil-based fungi community may have collaborated in decomposing the added straw tissues.

The relative abundances of the fungi phyla of the ST, LE, SH and CK treatments are presented in Figure 3B. For Ascomycota (22.0–75.1%), Basidiomycota (18.4–66.4%) and Mortierellomycota (6.4–25.0%), the fungal communities were found to be dominant across all incubation periods. The relative abundance of the Ascomycota phylum in ST, LE and SH treatments decreased by 56.5%, 62.1% and 17.9%, while that of the Basidiomycota phylum increased by 76.3%, 129.6% and 34.2%, respectively, following the incubation time ($p < 0.05$). Compared with CK, the relative abundance of Ascomycota exhibited a significant increase of 37.0–50.5%, while that of Basidiomycota showed a notable decrease, ranging from 32.5% to 68.2% ($p < 0.05$). Throughout the incubation period, a similar trend in fungi community succession was observed among the ST, LE and SH treatments.

The fungi co-occurrence network patterns in the four treatments during the incubation periods are illustrated in Figure 4. The nodes within the fungal network mainly belong to Ascomycota and Basidiomycota.

The topological properties of the co-occurrence networks of ST, LE, SH and CK at different stages are listed in Table 3. The values of the average clustering coefficient (avgCC) and average degree (avgK) in the ST, LE and SH treatments increased by 14.9–49.9% and 24.8–33.8%, while they decreased by 70.0% and 91.4% in the CK treatment following the incubation stages. In the early stages, both avgK and avgCC, in the ST, LE and SH treatments, were lower compared to CK, while in the later stages, they were higher. GD was greater in the ST, LE and SH treatments than in CK but became lower in the later stages. The complexity of the fungi networks of the ST, LE and SH treatments increased, while that of CK decreased, over the incubation period. In addition, the application of straw tissues increased both the complexity and efficiency of the fungi network.

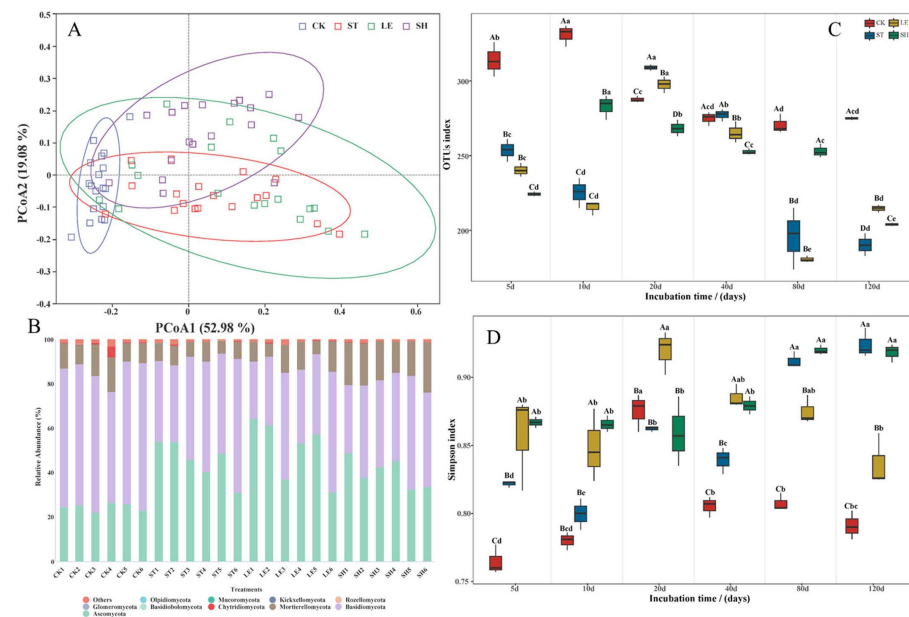


Figure 3. Effects of different straw tissues on the soil fungi community structure (A), relative abundance of the main abundant fungi phyla (B) and the OTU abundance (C) and Simpson indices (D) at different incubation stages. Fungi communities using principal coordinate analysis (PCoA) based on weighted UniFrac distances among all samples. Corresponding bars with different letters indicate significant differences ($p < 0.05$). The abundances of fungi communities are based on the corresponding proportional frequencies of ITS rRNA sequences. ST, maize straw stem; LE, maize straw leaves; SH, maize straw sheath; CK, the control without straw application.

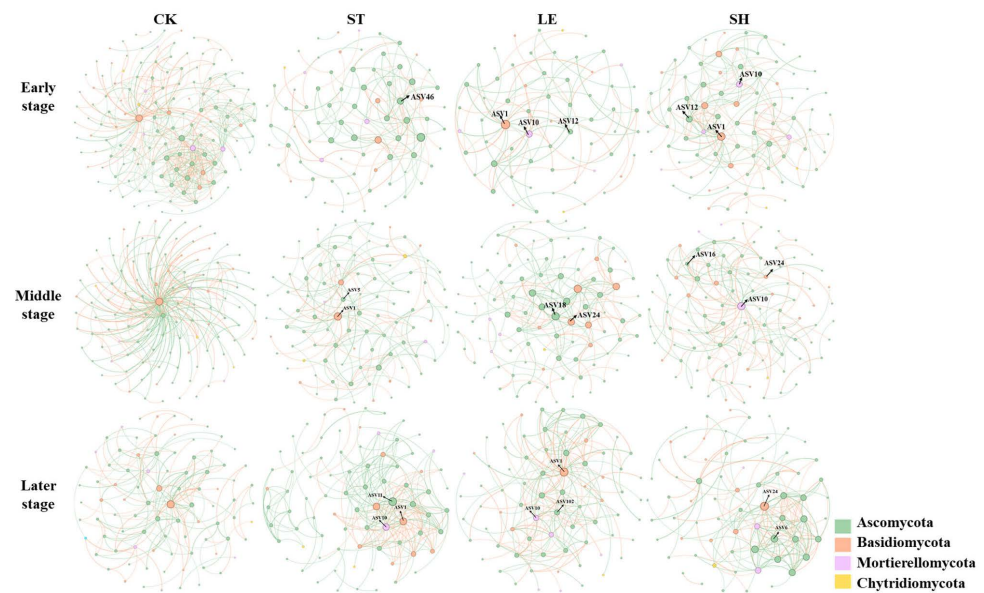


Figure 4. Fungi community co-occurrence in response to straw stem (ST), leaf (LE) and sheath (SH) amendment and control (CK) in the early, middle and later stages of incubation. The different colors of node indicate different phyla. The orange lines indicate negative interactions, while the green lines indicate positive interactions.

Distinct keystone taxa were identified from the fungi co-occurrence networks of different treatments, as shown in Table 4.

Table 3. The topological properties of the empirical networks of fungi communities under the straw tissues for stem (ST), leaf (LE) and sheath (SH) application and the control (CK).

Treatment	Node	Edge	Positive	Negative	Average Degree (avgK)	Diameter	Density	Modularity	Average Clustering Coefficient (avgCC)	Average Path Distance (GD)	Betweenness_Centralization	Degree_Centralization	
ST	Early	157	119	56.3	43.7	2.644	15	0.0097	0.706	0.3626	5.4129	0.0621	0.0544
	Middle	203	175	60.6	39.4	3.103	10	0.0085	0.631	0.2849	4.0872	0.0749	0.0855
	Later	193	247	66.8	33.2	5.277	10	0.0133	0.451	0.4929	3.6832	0.0427	0.1325
LE	Early	157	85	55.3	44.7	2.366	11	0.0069	0.621	0.2897	4.3958	0.0449	0.0764
	Middle	211	183	61.8	38.3	3.208	14	0.0083	0.62	0.4331	4.8536	0.0480	0.0584
	Later	129	187	52.9	47.1	4.456	7	0.0227	0.439	0.3850	3.0074	0.0774	0.1727
SH	Early	169	179	55.9	44.1	3.612	7	0.0126	0.616	0.3757	3.0385	0.0266	0.0886
	Middle	198	182	52.2	47.8	3.241	11	0.0093	0.608	0.2917	3.9736	0.0919	0.1125
	Later	126	164	60.4	39.6	4.245	9	0.0208	0.431	0.5655	3.7670	0.0625	0.1312
CK	Early	238	424	53.5	46.5	5.507	8	0.0150	0.56	0.4635	3.1973	0.1237	0.1369
	Middle	145	218	57.3	42.7	3.559	7	0.0209	0.441	0.0994	2.6351	0.4478	0.5000
	Later	151	162	56.2	43.8	3.239	8	0.0143	0.621	0.2421	3.9261	0.0999	0.1324

Table 4. The keystone taxa associated with straw tissue decomposition at different incubation stages.

Treatments	Keystone Taxa	Degree	Kingdom	Phylum	Class	Order	Family	Genus	Species	VIP Score of EEA	
ST	early	ASV46	8	Fungi	Ascomycota	Sordariomycetes	Hypocreales	Nectriaceae	Nectria	Nectria_ramulariae	1.58713
	middle	ASV1	19	Fungi	Basidiomycota	Tremellomycetes	Cystofilobasidiales	Mrakiaceae	Tausonia	Tausonia_pullulans	2.01394
		ASV5	9	Fungi	Ascomycota	Sordariomycetes	Sordariales	Lasiochaeraceae	Schizothecium	Schizothecium_miniglutinans	1.93246
	later	ASV1	24	Fungi	Basidiomycota	Tremellomycetes	Cystofilobasidiales	Mrakiaceae	Tausonia	Tausonia_pullulans	1.93993
		ASV10	22	Fungi	Mortierellomycota	Mortierellomycetes	Mortierellales	Mortierellaceae	Mortierella	Mortierella_alpina	1.99996
		ASV11	28	Fungi	Ascomycota	Eurotiomycetes	Eurotiales	Trichocomaceae	Talaromyces	Talaromyces_purpureogenus	1.62333
LE	early	ASV1	13	Fungi	Basidiomycota	Tremellomycetes	Cystofilobasidiales	Mrakiaceae	Tausonia	Tausonia_pullulans	1.33279
	middle	ASV10	9	Fungi	Mortierellomycota	Mortierellomycetes	Mortierellales	Mortierellaceae	Mortierella	Mortierella_alpina	1.53937
		ASV12	6	Fungi	Ascomycota	Dothideomycetes	Pleosporales	Leptosphaeriaceae	Leptosphaeria	Leptosphaeria_sclerotoides	1.51172
	later	ASV18	14	Fungi	Ascomycota	Sordariomycetes	Sordariales	Chaetomiaceae	Botryotrichum	Botryotrichum_atrogriseum	1.92881
		ASV24	12	Fungi	Basidiomycota	Tremellomycetes	Cystofilobasidiales	Mrakiaceae	Mrakia	Mrakia_frigida	1.83323
	ASV1	25	Fungi	Basidiomycota	Tremellomycetes	Cystofilobasidiales	Mrakiaceae	Tausonia	Tausonia_pullulans	1.93993	
SH	early	ASV10	15	Fungi	Mortierellomycota	Mortierellomycetes	Mortierellales	Mortierellaceae	Mortierella	Mortierella_alpina	1.99996
	middle	ASV102	14	Fungi	Ascomycota	Sordariomycetes	Hypocreales	Stachybotryaceae	Striatibotrys	Striatibotrys_eucylindrospora	1.82102
		ASV1	17	Fungi	Basidiomycota	Tremellomycetes	Cystofilobasidiales	Mrakiaceae	Tausonia	Tausonia_pullulans	1.33279
	later	ASV10	12	Fungi	Mortierellomycota	Mortierellomycetes	Mortierellales	Mortierellaceae	Mortierella	Mortierella_alpina	1.53937
		ASV12	13	Fungi	Ascomycota	Dothideomycetes	Pleosporales	Leptosphaeriaceae	Leptosphaeria	Leptosphaeria_sclerotoides	1.51172
	ASV10	24	Fungi	Mortierellomycota	Mortierellomycetes	Mortierellales	Mortierellaceae	Mortierella	Mortierella_alpina	2.20626	

Note: ST represents the stems tissues of maize straw; LE represents the leaf tissues of maize straw; SH represent the sheath tissues of maize straw.

3.4. Changes in EEA Activity with Decomposition

The activities of the POD, PPO, β GC and β X enzymes are shown in Figure 5. The activity of the POD enzyme decreased, while that of the β X enzyme increased, during the incubation time ($p < 0.05$). And the activities of the β GC and β X enzymes in the ST, LE and SH treatments were greater compared to the CK treatment ($p < 0.05$).

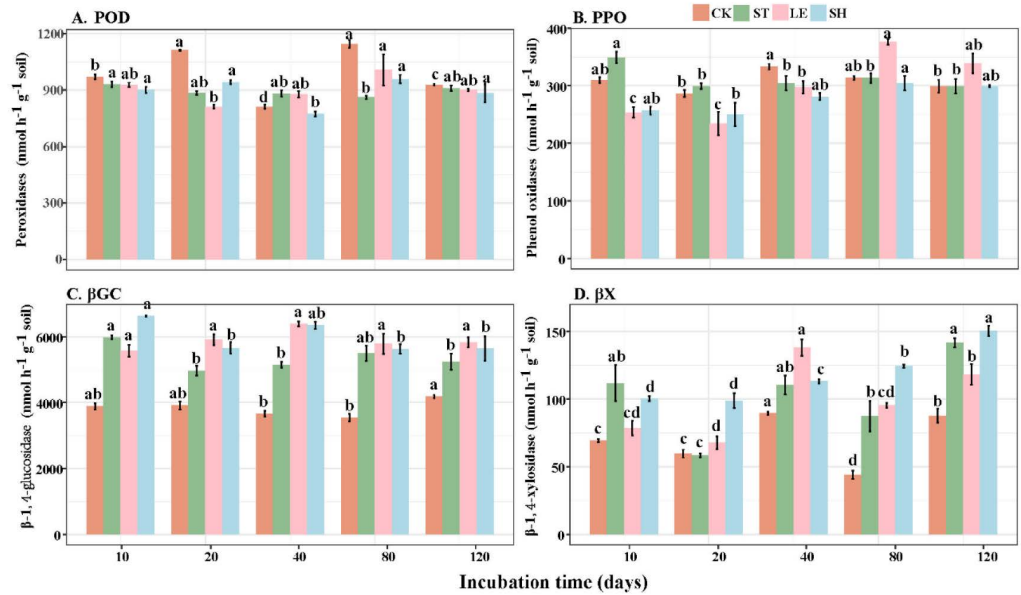


Figure 5. Extracellular enzyme activity in maize straw tissue stem (ST), leaf (LE), sheath (SH) application and the control (CK) after decomposition. Lowercase letters indicate significant differences between sampling stages.

The relative importance levels of the keystone taxa in the four extracellular enzymes were evaluated using random forest, as shown in Figure 6. The relative abundance of keystone taxa belonging to the Class *Dothideomycetes* and *Sordariomycetes* emerged as a primary determinant of the main determinants of oxidase activities. Furthermore, the relative abundances of keystone taxa from the classes *Tremellomycetes* and *Mortierellomycetes* emerged as a key determinant of the main determinants of hydrolase activities.

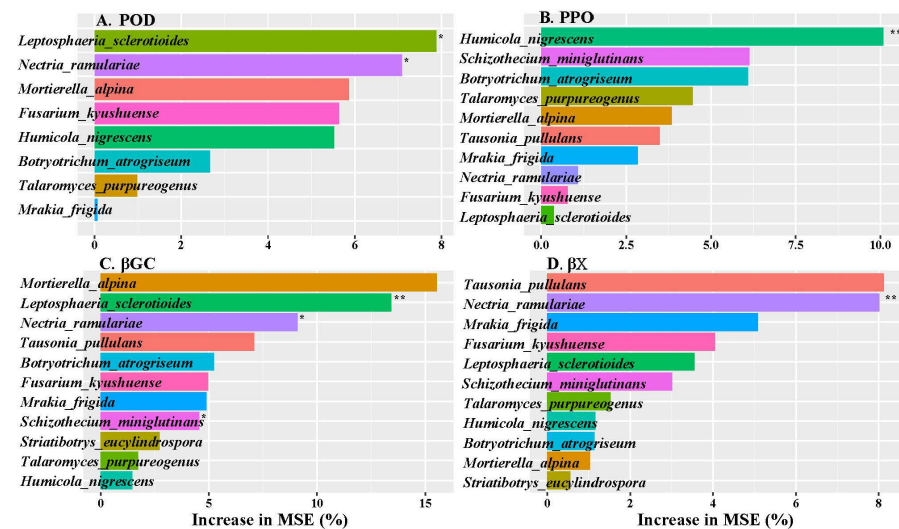


Figure 6. The importance of keystone taxa in the extracellular enzyme activity of POD (A), PPO (B), β GC (C) and β X (D) enzymes. ** represented $p < 0.01$; * represented $p < 0.05$.

3.5. The Correlation Analysis

The soil fungi community composition was separated into two main groups via MRT analysis based on the di-O-alkyl C content (20.0% of the variation in the fungi community composition was explained by this split). The SH treatment showed a higher relative content of di-O-alkyl C (Figure 7A). Further separation between the ST and LE treatments was determined by their relative contents of carbonyl C, with the LE treatment exhibiting a higher relative carbonyl-C content ($\geq 10.75\%$) compared to ST treatments. The EEA activities explained 95.0% of total variance in the C chemical structure. The PPO (74.7%, $p = 0.001$) was identified as the most crucial variable in forward selection, followed by βX (37.0%, $p < 0.05$). Additionally, we also used RDA for EEA activities as response variables and fungi keystone taxa as explanatory factors. Meanwhile, RDA1 and RDA2 accounted for 88.4% and 7.1%, respectively, of the total variance in the EEA activities when we used RDA for EEA activities as the response variable and fungi keystone taxa as the explanatory factors. The ASV12 (66.9%, $p = 0.001$) was identified as the most crucial variable in forward selection, followed by ASV10 (62.1%, $p = 0.001$) and ASV46 (54.7%, $p = 0.001$). In addition, RDA1 and RDA2 accounted for 57.3% and 31.2%, respectively, of the total variance in the C structure (Figure 7D). The ASV11 (60.2%, $p = 0.003$) was identified as the most crucial variable in the fungi keystone taxa.

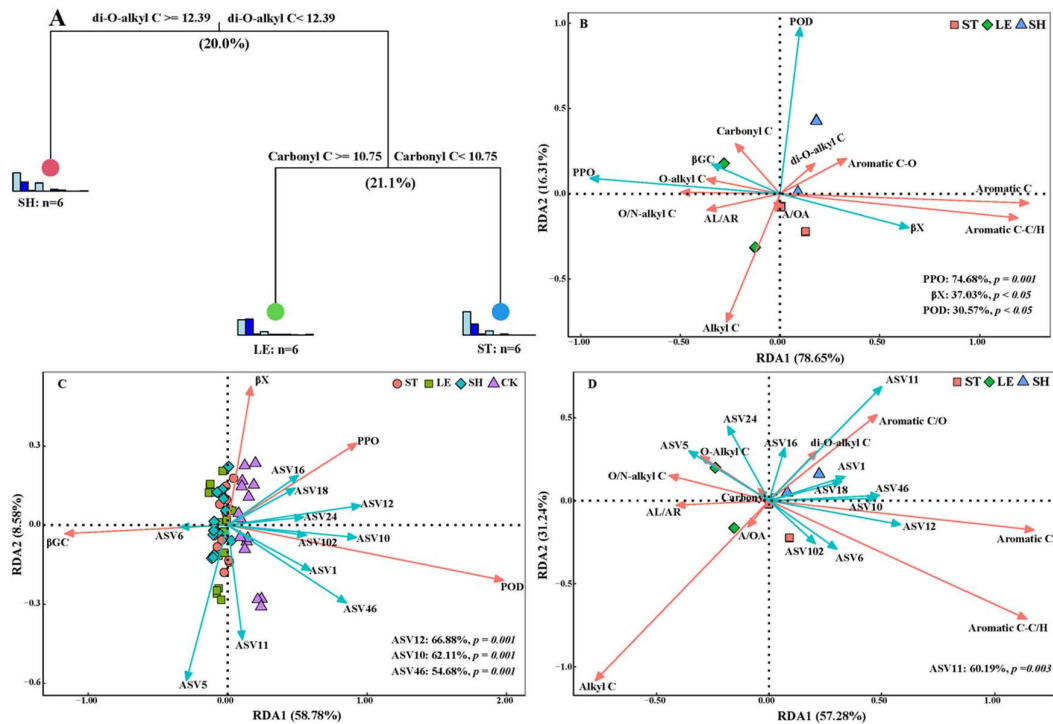


Figure 7. The multivariate regression tree (MRT) for the fungi community at the genus level (A). The variation explained at each split of the MRT is shown as a percentage in parentheses in the body of each branch. The redundancy analysis (RDA) correlation plot shows variance in the C structures of straw tissue stems (ST), leaves (LE) and sheaths (SH) as affected by extracellular enzyme activity (B) and the fungi keystone taxa (D), as well as extracellular enzyme activity as affected by fungi keystone taxa (C).

Structural equation modeling (SEM) was employed to assess the factors affecting the degradation of straw stems, leaves and sheaths, as shown in Figure 8. In the ST treatments, the A/OA ratio was positive linked with *Fusarium_kyushuense* abundance, while it was negatively associated with βGC activity. Furthermore, in the SH treatments, the POD activity exhibited a positive relationship with *Fusarium_kyushuense* abundance. The A/OA ratio displayed a negative correlation with POD activity but showed a positive

link with *Striatibotrys_eucylindrospora* abundance. This suggests that the keystone taxa and extracellular enzyme activity played important roles in straw tissue decomposition.

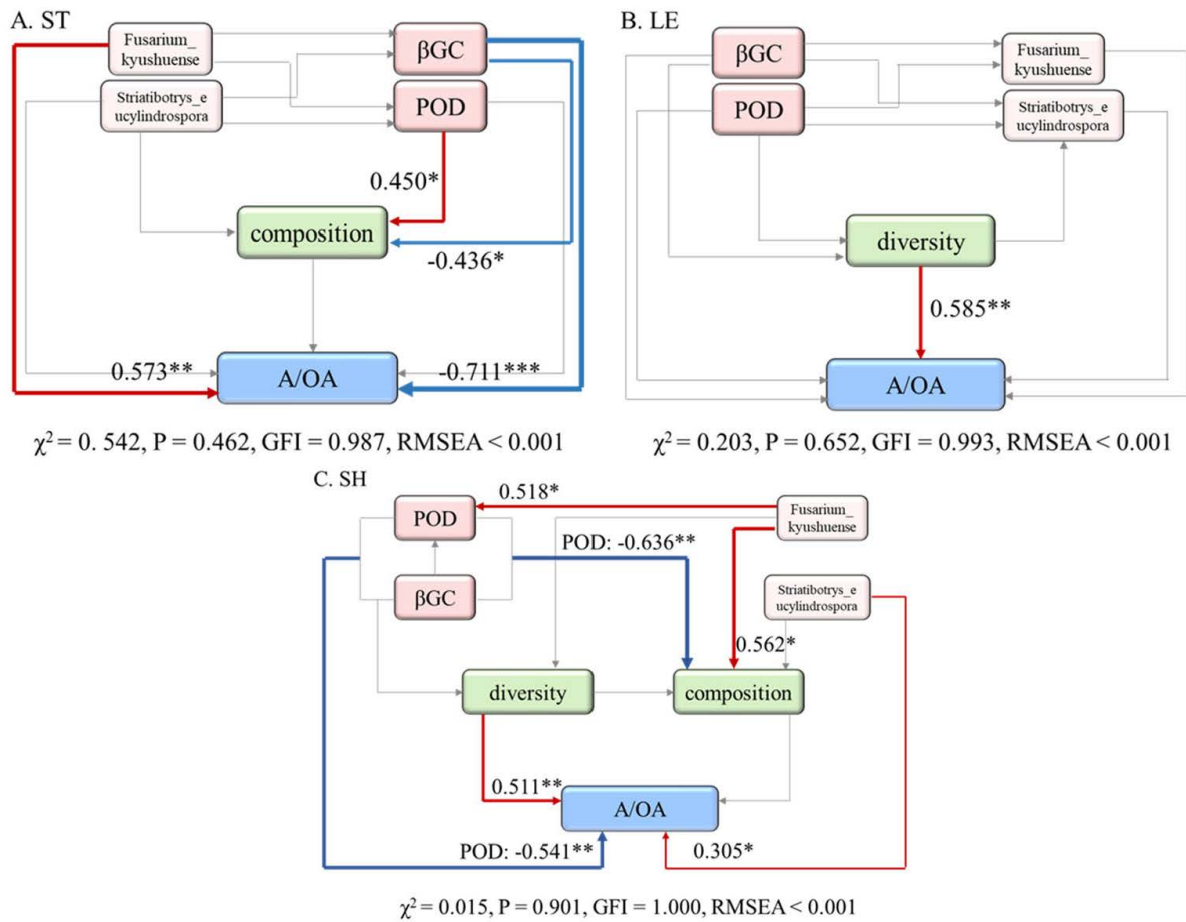


Figure 8. The effects of abiotic and biotic factors on the residue decomposition proportions of (A) ST, (B) LE and (C) SH, as estimated using the structural equation model (SEM). Path coefficients are shown by the numbers next to arrows. The strength of the standardized path coefficient is shown by the width of the arrows. Positive path coefficients are represented by red lines, negative path coefficients are represented by blue lines and non-coefficients are represented by grey lines. Significance levels are denoted with * $p < 0.05$, ** $p < 0.01$ and *** $p < 0.001$. Fungi community composition diversity is represented by the first axis of PCA; *Fusarium_kyushuense* and *Striatibotrys_eucylindrospora* were the keystone taxa. POD and β GC were extracellular enzymes.

According to FunGuild functional predictions, the fungi community functions predicted in the ST, LE, SH and CK treatments were analyzed (Figure 9). The potential functions related to Plant_Pathogen-Soil_Saprotroph-Wood_Saprotroph were significantly higher ($p < 0.05$) in the ST, LE and SH treatments compared with CK. Potential bacterial functions, such as Dung_Saprotroph, were significantly higher in the SH treatment compared to the ST treatment ($p < 0.05$).

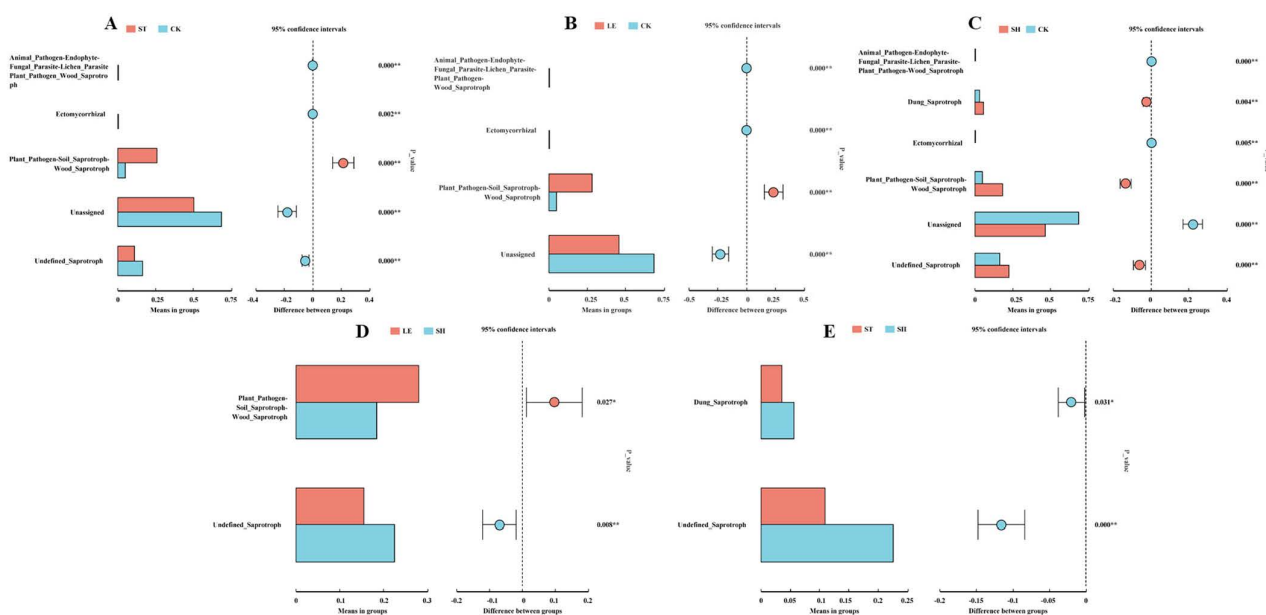


Figure 9. The potential fungi functions based on FunGuild between different treatment groups, including the CK, ST, LE and SH treatments. (A). the potential fungi functions based on FunGuild between ST and CK; (B). the potential fungi functions based on FunGuild between LE and CK; (C). the potential fungi functions based on FunGuild between SH and CK; (D). the potential fungi functions based on FunGuild between LE and SH; (E). the potential fungi functions based on FunGuild between ST and SH. * $p < 0.05$, ** $p < 0.01$.

4. Discussion

4.1. Difference of Chemical Structure in Straw Tissue

The decomposition process of straw tissues can be divided into two stages, an initial rapid loss followed by the slower loss (Figure 1). This phenomenon can be attributed to the presence of easily decomposable compounds of straw tissues with during the initial stage, while recalcitrant compounds degrade more slowly in the later stages [2,49]. Similar findings have been reported in other studies, such as the rapid decomposition of maize residue within the first two months, followed by a decrease in the decomposition rate r [22]. Additionally, the straw stem and leaf tissues showed higher decomposition proportions compared to straw sheath tissue (Figure 1). Mwafulirwa et al. (2019) also found that ryegrass root residues mineralize at a slower rate than shoot residues [13]. This result could be explained by the differences in the C/N ratio among residue types, where lower a C/N ratio is associated with faster decomposition rates compared to higher C/N ratios [1,50]. For example, *Liangyu99* maize stover with a lower C/N ratio had a higher decomposition rate compared with *Xianyu335* maize [50]. This is also consistent with the study of Xu et al. (2017) showing that soybean residues with lower C/N ratios experienced greater mass loss compared with wheat residues that had a greater C/N ratio [1].

The NMR data in our study revealed that the chemical structure of straw changed from 80 d to 120 d across the three treatments (Table 2). Irrespective of the straw tissues or incubation stages, O-alkyl C was found to be the dominant component in the chemical composition of straw. This finding aligns with those of previous studies indicating that O-alkyl C is usually a major constituent of the most abundant compound cellulose of residues [1,51]. Our results demonstrated an increase in the relative proportion of alkyl C and a decrease in O-alkyl C within the three treatments from 80 d to 120 d. The decline observed in O-alkyl C may be due to its inclusion of the labile C compound, which is preferentially consumed by microorganisms to degrade a recalcitrant structure [2]. Meanwhile, the increase observed in alkyl C content can be explained by its inclusion of recalcitrant components that are hard to degrade and the transformation of labile C into structural

microbial C [52]. These findings indicate that straw stems, leaves and sheaths undergo decomposition over time, and this is further supported by the higher alkyl C/O-alkyl C ratio (A/OA) observed at 120 d compared to 80 d across all three treatments. A greater A/OA ratio indicates increased decomposition of crop residues [53].

O-alkyl C and di-O-alkyl C, primarily associated with cellulose and hemicellulose [1], exhibited greater decomposition in straw stem and leaves than in sheath residues. On the other hand, the A/OA ratios of straw stem and leaf treatments were higher than that of sheath treatment, regardless of the incubation time, indicating that a higher degree of decomposition occurs in stems and leaves relative to sheaths. Aromatic C constitutes a major component of tannin and lignin [54], and it is found in a higher proportion in straw sheaths compared to stems and leaves. This may be due to the slowest decomposition degree of straw sheaths. Overall, we found that the decomposition of crop residues from stems, leaves and sheaths were accompanied by relative decreases in reactive O-alkyl C and di-O-alkyl C contents, as well as relative increases in recalcitrant C, such as aromatic C, and alkyl C.

4.2. Difference of Fungi Community Composition

The application of straw stems, leaves and sheaths into soil resulted in a decrease in the OTUs of the fungi community (Figure 3), which is consistent with other studies [55,56]. This can be explained by the following reasons: (1) the stimulation of a subset of the microbial community specializing in the degradation of straw tissues; (2) the soil used in our study had a lower C/N ratio, limiting carbon availability for microbial growth; (3) functional redundancy is prevalent within the microbial system during residue decomposition, where multiple microbial components with similar functions occupy the same ecological niche [22,57].

The PCoA and relative abundance analysis suggested that the fungi community compositions were similar among the treatments with straw stem, leaf and sheath applications (Figure 3), which was inconsistent with other studies [30,58,59]. For example, Li et al. (2020) found that the microbial community composition changed greatly after wheat residues' incorporation into soil [2]. Similarly, other studies also showed that the addition of organic amendments in agricultural soils can affect fungal community compositions [29]. The discrepancy may be attributed to the narrow range of residues used in our study, which were different tissues in the same maize straw. The initial soil fungi communities of the four treatments were predominantly composed of Ascomycota, Basidiomycota, Mortierellomycota and Chytridiomycota (Figure 3). Notably, the application of straw tissues increased the relative abundance of Ascomycota compared with the control. This could be explained by the fact that Ascomycota is a copiotrophic population (r-strategy) stimulated by decomposable residue compounds during the early stages of residue decomposition [22,60]. *Fusarium_solani* and *Fusarium_kyushuense* species showed similar changes to phylum Ascomycota. A recent study also found that the genus of *Fusarium* was stimulated by litter, and cultured representative isolates of this taxon were shown to have decomposing ability [61,62].

Furthermore, the fungi community composition exhibited time-dependent trends as straw decomposition progressed. The fungal phylum Ascomycota dominated the fungi community composition relative to other taxa during the early stages (Figure 3), which was consistent with previous studies [22,29,31]. Ascomycota is a copiotrophic population (r-strategy) stimulated by decomposable residue compounds during the initial stages of residue decomposition [63]; Voriskova and Baldrian (2013) found that fungal phylum Ascomycota was prevalent in live and senescent leaves on the trees, accounting for more than 88% of the abundance during litter decomposition [60]. The classes of *Sordariomycetes*, *Dothideomycetes* and *Eurotiomycetes* showed similar succession trajectories to the Ascomycota phylum, which was in agreement with other studies [1,8]. Another study also found that Ascomycota decreased during the process of degradation as the Basidiomycota phylum gradually increased [64], which indicated that the Basidiomycota phylum plays a role in

degrading the recalcitrant carbon. Other research also proved that members of the phylum Basidiomycota are capable of decomposing recalcitrant substrates such as lignin and humic substances, becoming dominant during the later decomposition stages [63]. Moreover, the fungal Basidiomycetes could utilize hydrolytic enzymes typically composed of β GC to degrade residue carbohydrates and cellulose for meeting fungal C demand for their growth, as reflected by high activity of β GC enzymes during the initial stages of straw tissue decomposition [22,65]. However, due to the limited observation period of four months used in our study, we are unable to fully capture the complete fungal succession related to litter chemistry dynamics over a long-term period. This highlights the necessity for prolonged, longitudinal, multispecies experiments that can elucidate the connection between specific molecular traits of litter and the occurrence, as well as persistence, of climax microbials.

4.3. Linkages between Chemical Structure, EEA Activities and Fungi Composition

During the decomposition stage, we observed a significant relationship between the chemical structures of residues, EEA activity and fungi composition (Figure 8). The fungi community composition was primarily determined by di-O-alkyl C and carbonyl-C contents during the straw stem, leaf and sheath decomposition processes (Figure 8). Li et al. (2020) found that the compositions of the main microbial groups during the straw decomposition were mainly influenced by the alkyl C and N-alkyl/methoxyl C contents of wheat straw and the O-alkyl C and di-O-alkyl C contents of maize straw [2]. Our results indicated that the carbohydrate content strongly influenced the compositions of the main fungi groups involved in decomposing various tissues of maize stover.

In the decomposition processes of straw stems, leaves and sheaths, the keystone taxa abundances, such as *Fusarium_kyushuense* and *Striatibotrys_eucylindrospora*, showed strong negative associations with di-O-alkyl C and carbonyl-C contents, while they were positively associated with aromatic C and aromatic C-C/H (Figure 8), which suggests that these keystone taxa are involved in the degradation of carbohydrates and accumulation of aromatic substances. Previous studies also indicated the importance of keystone taxa like *Fusarium_kyushuense* of the genera *Fusarium* in microbial litter decomposition due to their the strong decomposition ability and enzyme activities [39,59]. The keystone taxa of *Fusarium_kyushuense* and *Striatibotrys_eucylindrospora* belong to the class of *Sordariomycetes* (Table 3). It has been reported that *Sordariomycetes* are predominantly involved in cellulose utilization and substantially affect the assimilation of C from plant residues [29,66–68], which is consistent with previous studies showing *Sordariomycetes* to be one of the largest classes in phylum Ascomycota, ubiquitous in agricultural soils due to its high capacity for utilizing labile carbon resources [69]. And Koechli et al. (2019) performed high-throughput sequencing that enabled stable isotope probing (HTS-SIP) to prove that the class *Sordariomycetes* participates in exogenous-C assimilation [70].

Soil enzymes are the primary drivers of plant residue degradation by fungi in most ecosystems [43]. In our study, the keystone taxa, *Fusarium_kyushuense* and *Striatibotrys_eucylindrospora*, were positively associated with β GC and POD enzyme activity, respectively (Figure 8), indicating their involvement in the secretion of extracellular enzymes. It is also reported that *Fusarium* produce ligninolytic peroxidases, which are essential enzymes for lignin degradation [71,72]. Furthermore, Zheng et al. (2021) confirmed that fungal keystone taxa, such as *Fusarium* sp., exhibit higher rates of decomposition and enzyme activity [39]. Thus, it is worth analyzing hydrolases and oxidases produced by these keystone taxa in future work. Oates et al. (2021) also discovered the widespread distribution of carbohydrate-active enzymes among lignocellulose-degrading fungi from *Sordariomycetes* [73].

Previous studies have suggested that the changes in the soil microbial community and enzyme activities were primarily attributed to the greatest extent of the SOC chemical structure [74,75]. Our study also revealed significant correlations between the chemical structures of crop residues, extracellular enzyme activities and the relative abundances of

the keystone taxa in our study (Figure 8). The positive association between β GC and POD activity, as well as between the carbonyl C and O-alkyl C contents, indicated that these enzymes are involved in the degradation of active C. β GC plays a crucial role in catalyzing the hydrolysis and biodegradation of cellulose, leading to glucose production, which serves as an important energy source for soil microorganisms' growth and activity [76]. In addition, a study suggested that fungi have evolved extracellular oxidative enzymes to oxidize lignin and convert its aromatic constituents [77], which is consistent with our results highlighting a negative association between oxidase activity (POD) and aromatic C.

The SEM analysis conducted in our study also suggested that the presence of keystone taxa and EEA activity played an important role in straw tissue decomposition (Figure 9). In general, the degradation process primarily involves the breakdown of di-O-alkyl C and carbonyl-C through extracellular enzymes secreted by these keystone taxa.

5. Conclusions

Our study suggests that the decomposition processes of different straw tissues undergo chemical structure transformation accompanied by a similar succession of fungi community. In the early stages, the fungal community composition is dominated by the Ascomycota phylum, while in the later stages, it is dominated by Basidiomycetous. The degree of decomposition in straw leaves was greater than that in the stems and sheaths at the end of the incubation time. Furthermore, we have identified the keystone taxa of fungi that play a crucial role in driving chemical structure transformation during straw tissue degradation. The class of *Sordariomycetes* was found to be the main contributor to the straw tissue chemistry transformation of decomposition through its influence on the secretions and activities of β -glucosidase and peroxidase. In summary, our study demonstrated the great importance of fungi keystone taxa for straw decomposition and provided new perspectives for understanding the inter-relationship between residue decomposition, fungi keystone taxa and extracellular enzyme function, and it helped us to further understand SOC sequestration.

Supplementary Materials: The following supporting information can be downloaded at: <https://www.mdpi.com/article/10.3390/agriculture14060792/s1>, Table S1: The basic characteristic of soil use in this experiment; Table S2: A one-way ANOVA was used to determine the statistical significance of the effect of factors (1) straw tissues and (2) incubation stage on the proportion of straw decomposition.

Author Contributions: X.L. (Xiujun Li) and X.L. (Xinrui Lu) designed the experiment; Q.Z. performed all the experiments; Q.Z. analyzed the data and wrote the manuscript; X.L. (Xiujun Li), X.L. (Xinrui Lu), G.C., N.L. and J.S. provided comments and revised the manuscript. X.L. (Xiujun Li) and X.L. (Xinrui Lu) provide the funding required to conduct this study. E.A.N. provide editorial assistance. All authors have read and agreed to the published version of the manuscript.

Funding: This research was supported by National Key Research and Development Program of China (No. 2023YFD1500703), the Strategic Priority Research Program of the Chinese Academy of Sciences (No. XDA28020401, XDA23070500), National Science Foundation of China (No. 41877024).

Institutional Review Board Statement: Not applicable.

Data Availability Statement: The data that support the findings of this study are available upon request from the corresponding author. The data are not publicly available due to privacy or ethical restrictions.

Acknowledgments: Besides financial support, we, the authors, would like to acknowledge the support of all involved persons and employees involved in the research tasks, without whom this project would not have been possible.

Conflicts of Interest: The authors declare no conflicts of interest.

References

1. Xu, Y.; Chen, Z.; Fontaine, S.; Wang, W.; Luo, J.; Fan, J.; Ding, W. Dominant effects of organic carbon chemistry on decomposition dynamics of crop residues in a Mollisol. *Soil Biol. Biochem.* **2017**, *115*, 221–232. [[CrossRef](#)]
2. Li, D.; Li, Z.; Zhao, B.; Zhang, J. Relationship between the chemical structure of straw and composition of main microbial groups during the decomposition of wheat and maize straws as affected by soil texture. *Biol. Fertil. Soils* **2020**, *56*, 11–24. [[CrossRef](#)]
3. Lal, R. Soil carbon sequestration impacts on global climate change and food security. *Science* **2004**, *304*, 1623–1627. [[CrossRef](#)] [[PubMed](#)]
4. Wahdan, S.F.M.; Ji, L.; Schadler, M.; Wu, Y.-T.; Sansupa, C.; Tanunchai, B.; Buscot, F.; Purahong, W. Future climate conditions accelerate wheat straw decomposition alongside altered microbial community composition, assembly patterns, and interaction networks. *ISME J.* **2023**, *17*, 238–251. [[CrossRef](#)] [[PubMed](#)]
5. Liu, D.; Keiblinger, I.M.; Leitner, S.; Mentler, A.; Zechmeister-Boltenstern, S. Is there a convergence of deciduous leaf litter stoichiometry, biochemistry and microbial population during decay? *Geoderma* **2016**, *272*, 93–100. [[CrossRef](#)]
6. Wang, H.; Liu, S.; Wang, J.; Shi, Z.; Lu, L.; Guo, W.; Jia, H.; Cai, D. Dynamics and speciation of organic carbon during decomposition of leaf litter and fine roots in four subtropical plantations of China. *For. Ecol. Manag.* **2013**, *300*, 43–52. [[CrossRef](#)]
7. Tharayil, N.; Suseela, V.; Triebwasser, D.J.; Preston, C.M.; Gerard, P.D.; Dukes, J.S. Changes in the structural composition and reactivity of *Acer rubrum* leaf litter tannins exposed to warming and altered precipitation: Climatic stress-induced tannins are more reactive. *New Phytol.* **2011**, *191*, 132–145. [[CrossRef](#)] [[PubMed](#)]
8. Huang, F.; Li, Q.; Xue, L.; Han, J.; Zamanian, K.; Zhao, X. The succession of microbial communities after residue returning in a Solonchak. *Plant Soil* **2023**, *492*, 191–208. [[CrossRef](#)]
9. Han, Y.; Yao, S.-H.; Jiang, H.; Ge, X.-I.; Zhang, Y.; Mao, J.; Dou, S.; Zhang, B. Effects of mixing maize straw with soil and placement depths on decomposition rates and products at two cold sites in the mollisol region of China. *Soil Tillage Res.* **2020**, *197*, 104519. [[CrossRef](#)]
10. Wang, X.; Sun, B.; Mao, J.; Sui, Y.; Cao, X. Structural Convergence of Maize and Wheat Straw during Two-Year Decomposition under Different Climate Conditions. *Environ. Sci. Technol.* **2012**, *46*, 7159–7165. [[CrossRef](#)]
11. Thongjoo, C.; Miyagawa, S.; Kawakubo, N. Effects of soil moisture and temperature on decomposition rates of some waste materials from agriculture and agro-industry. *Plant Prod. Sci.* **2005**, *8*, 475–481. [[CrossRef](#)]
12. Seyfried, G.S.; Dalling, J.W.; Yang, W.H. Mycorrhizal type effects on leaf litter decomposition depend on litter quality and environmental context. *Biogeochemistry* **2021**, *155*, 21–38. [[CrossRef](#)]
13. Mwafurirwa, L.; Baggs, E.M.; Morley, N.; Paterson, E. Ryegrass root and shoot residues differentially affect short-term priming of soil organic matter and net soil C-balance. *Eur. J. Soil Biol.* **2019**, *93*, 103096. [[CrossRef](#)]
14. Su, Y.; Gong, Y.; Han, W.; Li, K.; Liu, X. Dependency of litter decomposition on litter quality, climate change, and grassland type in the alpine grassland of Tianshan Mountains, Northwest China. *J. Arid Land* **2022**, *14*, 691–703. [[CrossRef](#)]
15. Pascault, N.; Cecillon, L.; Mathieu, O.; Henault, C.; Sarr, A.; Leveque, J.; Farcy, P.; Ranjard, L.; Maron, P.-A. In Situ Dynamics of Microbial Communities during Decomposition of Wheat, Rape, and Alfalfa Residues. *Microb. Ecol.* **2010**, *60*, 816–828. [[CrossRef](#)]
16. Clemente, J.S.; Simpson, M.J.; Simpson, A.J.; Yanni, S.F.; Whalen, J.K. Comparison of soil organic matter composition after incubation with maize leaves, roots, and stems. *Geoderma* **2013**, *192*, 86–96. [[CrossRef](#)]
17. Bertrand, I.; Chabbert, B.; Kurek, B.; Recous, S. Can the biochemical features and histology of wheat residues explain their decomposition in soil? *Plant Soil* **2006**, *281*, 291–307. [[CrossRef](#)]
18. Liu, J.; Ding, C.; Zhang, W.; Wei, Y.; Zhou, Y.; Zhu, W. Litter mixing promoted decomposition rate through increasing diversities of phyllosphere microbial communities. *Front. Microbiol.* **2022**, *13*, 1009091. [[CrossRef](#)] [[PubMed](#)]
19. Wickings, K.; Grandy, A.S.; Reed, S.C.; Cleveland, C.C. The origin of litter chemical complexity during decomposition. *Ecol. Lett.* **2012**, *15*, 1180–1188. [[CrossRef](#)]
20. Li, D.; Zhao, B.; Olk, D.C.; Zhang, J. Soil texture and straw type modulate the chemical structure of residues during four-year decomposition by regulating bacterial and fungal communities. *Appl. Soil Ecol.* **2020**, *155*, 103664. [[CrossRef](#)]
21. Nair, A.; Ngouajio, M. Soil microbial biomass, functional microbial diversity, and nematode community structure as affected by cover crops and compost in an organic vegetable production system. *Appl. Soil Ecol.* **2012**, *58*, 45–55. [[CrossRef](#)]
22. Zhao, S.; Fan, F.; Qiu, S.; Xu, X.; He, P.; Ciampitti, I.A. Dynamic of fungal community composition during maize residue decomposition process in north-central China. *Appl. Soil Ecol.* **2021**, *167*, 104057. [[CrossRef](#)]
23. Paterson, E.; Sim, A.; Osborne, S.M.; Murray, P.J. Long-term exclusion of plant-inputs to soil reduces the functional capacity of microbial communities to mineralise recalcitrant root-derived carbon sources. *Soil Biol. Biochem.* **2011**, *43*, 1873–1880. [[CrossRef](#)]
24. Cho, H.; Kim, M.; Tripathi, B.; Adams, J. Changes in Soil Fungal Community Structure with Increasing Disturbance Frequency. *Microb. Ecol.* **2017**, *74*, 62–77. [[CrossRef](#)] [[PubMed](#)]
25. Golebiewski, M.; Tarasek, A.; Sikora, M.; Deja-Sikora, E.; Tretyn, A.; Niklinska, M. Rapid Microbial Community Changes During Initial Stages of Pine Litter Decomposition. *Microb. Ecol.* **2019**, *77*, 56–75. [[CrossRef](#)] [[PubMed](#)]
26. Qiao, Y.-F.; Miao, X.-C.; Burger, M.; Miao, S.-J. Shift of fungal community composition in response to exogenous C application associated with soil properties after 10-year field experiment in black soil of China. *J. Soils Sediments* **2022**, *22*, 2281–2289. [[CrossRef](#)]

27. Lopez-Mondejar, R.; Brabcova, V.; Stursova, M.; Davidova, A.; Jansa, J.; Cajthaml, T.; Baldrian, P. Decomposer food web in a deciduous forest shows high share of generalist microorganisms and importance of microbial biomass recycling. *ISME J.* **2018**, *12*, 1768–1778. [[CrossRef](#)] [[PubMed](#)]
28. Xiao, D.; He, X.; Wang, G.; Xu, X.; Hu, Y.; Chen, X.; Zhang, W.; Su, Y.A.; Wang, K.; Soromotin, A.V.; et al. Network analysis reveals bacterial and fungal keystone taxa involved in straw and soil organic matter mineralization. *Appl. Soil Ecol.* **2022**, *173*, 104395. [[CrossRef](#)]
29. Veen, G.F.; ten Hoooven, F.C.; Weser, C.; Hannula, S.E. Steering the soil microbiome by repeated litter addition. *J. Ecol.* **2021**, *109*, 2499–2513. [[CrossRef](#)]
30. Baumann, K.; Marschner, P.; Smernik, R.J.; Baldock, J.A. Residue chemistry and microbial community structure during decomposition of eucalypt, wheat and vetch residues. *Soil Biol. Biochem.* **2009**, *41*, 1966–1975. [[CrossRef](#)]
31. Bonanomi, G.; De Filippis, F.; Cesarano, G.; La Stora, A.; Zotti, M.; Mazzoleni, S.; Incerti, G. Linking bacterial and eukaryotic microbiota to litter chemistry: Combining next generation sequencing with C-13 CPMAS NMR spectroscopy. *Soil Biol. Biochem.* **2019**, *129*, 110–121. [[CrossRef](#)]
32. Eichlerova, I.; Homolka, L.; Zifcakova, L.; Lisa, L.; Dobiasova, P.; Baldrian, P. Enzymatic systems involved in decomposition reflects the ecology and taxonomy of saprotrophic fungi. *Fungal Ecol.* **2015**, *13*, 10–22. [[CrossRef](#)]
33. Li, Y.; Nie, C.; Liu, Y.; Du, W.; He, P. Soil microbial community composition closely associates with specific enzyme activities and soil carbon chemistry in a long-term nitrogen fertilized grassland. *Sci. Total Environ.* **2019**, *654*, 264–274. [[CrossRef](#)]
34. Laza, H.E.; Acosta-Martinez, V.; Cano, A.; Baker, J.; Mahan, J.; Gitz, D.; Emendack, Y.; Slaughter, L.; Lascano, R.; Tissue, D.; et al. Elevated CO₂ enhances soil respiration and AMF abundance in a semiarid peanut agroecosystem. *Agric. Ecosyst. Environ.* **2023**, *355*, 108592. [[CrossRef](#)]
35. Sinsabaugh, R.L. Phenol oxidase, peroxidase and organic matter dynamics of soil. *Soil Biol. Biochem.* **2010**, *42*, 391–404. [[CrossRef](#)]
36. Purahong, W.; Krueger, D.; Buscot, F.; Wubet, T. Correlations between the composition of modular fungal communities and litter decomposition-associated ecosystem functions. *Fungal Ecol.* **2016**, *22*, 106–114. [[CrossRef](#)]
37. Peng, Y.; Li, Y.-j.; Song, S.-y.; Chen, Y.-q.; Chen, G.-t.; Tu, L.-h. Nitrogen addition slows litter decomposition accompanied by accelerated manganese release: A five-year experiment in a subtropical evergreen broadleaf forest. *Soil Biol. Biochem.* **2022**, *165*, 108511. [[CrossRef](#)]
38. Cusack, D.F.; Silver, W.L.; Torn, M.S.; Burton, S.D.; Firestone, M.K. Changes in microbial community characteristics and soil organic matter with nitrogen additions in two tropical forests. *Ecology* **2011**, *92*, 621–632. [[CrossRef](#)] [[PubMed](#)]
39. Zheng, H.; Yang, T.; Bao, Y.; He, P.; Yang, K.; Mei, X.; Wei, Z.; Xu, Y.; Shen, Q.; Banerjee, S. Network analysis and subsequent culturing reveal keystone taxa involved in microbial litter decomposition dynamics. *Soil Biol. Biochem.* **2021**, *157*, 108230. [[CrossRef](#)]
40. Gonzalez, A.; Germain, R.M.; Srivastava, D.S.; Filotas, E.; Dee, L.E.; Gravel, D.; Thompson, P.L.; Isbell, F.; Wang, S.; Kefi, S.; et al. Scaling-up biodiversity-ecosystem functioning research. *Ecol. Lett.* **2020**, *23*, 757–776. [[CrossRef](#)]
41. Banerjee, S.; Kirkby, C.A.; Schmutter, D.; Bissett, A.; Kirkegaard, J.A.; Richardson, A.E. Network analysis reveals functional redundancy and keystone taxa amongst bacterial and fungal communities during organic matter decomposition in an arable soil. *Soil Biol. Biochem.* **2016**, *97*, 188–198. [[CrossRef](#)]
42. Banerjee, S.; Schlaeppi, K.; van der Heijden, M.G.A. Keystone taxa as drivers of microbiome structure and functioning. *Nat. Rev. Microbiol.* **2018**, *16*, 567–576. [[CrossRef](#)] [[PubMed](#)]
43. Liao, H.; Xu, C.; Tan, S.; Wei, Z.; Ling, N.; Yu, G.; Raza, W.; Zhang, R.; Shen, Q.; Xu, Y. Production and characterization of acidophilic xylanolytic enzymes from *Penicillium oxalicum* GZ-2. *Bioresour. Technol.* **2012**, *123*, 117–124. [[CrossRef](#)] [[PubMed](#)]
44. Mei, N.; Zhang, X.; Wang, X.; Peng, C.; Gao, H.; Zhu, P.; Gu, Y. Effects of 40 years applications of inorganic and organic fertilization on soil bacterial community in a maize agroecosystem in northeast China. *Eur. J. Agron.* **2021**, *130*, 126332. [[CrossRef](#)]
45. Zhang, Q.; Lu, X.; Chen, G.; Luo, N.; Sun, J.; Li, X.; Ngozi, E.A. The priming effect patterns linked to the dominant bacterial keystone taxa during different straw tissues incorporation into Mollisols in Northeast China. *Appl. Soil Ecol.* **2024**, *197*, 105330. [[CrossRef](#)]
46. Shrestha, B.M.; Singh, B.R.; Forte, C.; Certini, G. Long-term effects of tillage, nutrient application and crop rotation on soil organic matter quality assessed by NMR spectroscopy. *Soil Use Manag.* **2015**, *31*, 358–366. [[CrossRef](#)]
47. Wang, X.; Liang, C.; Mao, J.; Jiang, Y.; Bian, Q.; Liang, Y.; Chen, Y.; Sun, B. Microbial keystone taxa drive succession of plant residue chemistry. *ISME J.* **2023**, *17*, 748–757. [[CrossRef](#)] [[PubMed](#)]
48. Baldock, J.A.; Masiello, C.A.; Gelinas, Y.; Hedges, J.I. Cycling and composition of organic matter in terrestrial and marine ecosystems. *Mar. Chem.* **2004**, *92*, 39–64. [[CrossRef](#)]
49. Grandy, A.S.; Salam, D.S.; Wickings, K.; McDaniel, M.D.; Culman, S.W.; Snapp, S.S. Soil respiration and litter decomposition responses to nitrogen fertilization rate in no-till corn systems. *Agric. Ecosyst. Environ.* **2013**, *179*, 35–40. [[CrossRef](#)]
50. Liu, S.; Fan, R.; Yang, X.; Zhang, Z.; Zhang, X.; Liang, A. Decomposition of maize stover varies with maize type and stover management strategies: A microcosm study on a Black soil (Mollisol) in northeast China. *J. Environ. Manag.* **2019**, *234*, 226–236. [[CrossRef](#)]
51. Xu, Y.; Fan, J.; Ding, W.; Gunina, A.; Chen, Z.; Bol, R.; Luo, J.; Bolan, N. Characterization of organic carbon in decomposing litter exposed to nitrogen and sulfur additions: Links to microbial community composition and activity. *Geoderma* **2017**, *286*, 116–124. [[CrossRef](#)]

52. Lundberg, P.; Ekblad, A.; Nilsson, M. C-13 NMR spectroscopy studies of forest soil microbial activity: Glucose uptake and fatty acid biosynthesis. *Soil Biol. Biochem.* **2001**, *33*, 621–632. [[CrossRef](#)]
53. Zhao, H.; Lv, Y.; Wang, X.; Zhang, H.; Yang, X. Tillage impacts on the fractions and compositions of soil organic carbon. *Geoderma* **2012**, *189*, 397–403. [[CrossRef](#)]
54. Lorenz, K.; Preston, C.M.; Raspe, S.; Morrison, I.K.; Feger, K.H. Litter decomposition and humus characteristics in Canadian and German spruce ecosystems: Information from tannin analysis and C-13 CPMAS NMR. *Soil Biol. Biochem.* **2000**, *32*, 779–792. [[CrossRef](#)]
55. Sanaullah, M.; Chabbi, A.; Maron, P.-A.; Baumann, K.; Tardy, V.; Blagodatskaya, E.; Kuzyakov, Y.; Rumpel, C. How do microbial communities in top-and subsoil respond to root litter addition under field conditions? *Soil Biol. Biochem.* **2016**, *103*, 28–38. [[CrossRef](#)]
56. Zhao, S.; Qiu, S.; Xu, X.; Ciampitti, I.A.; Zhang, S.; He, P. Change in straw decomposition rate and soil microbial community composition after straw addition in different long-term fertilization soils. *Appl. Soil Ecol.* **2019**, *138*, 123–133. [[CrossRef](#)]
57. Herzog, C.; Hartmann, M.; Frey, B.; Stierli, B.; Rumpel, C.; Buchmann, N.; Brunner, I. Microbial succession on decomposing root litter in a drought-prone Scots pine forest. *ISME J.* **2019**, *13*, 2346–2362. [[CrossRef](#)] [[PubMed](#)]
58. Pascault, N.; Ranjard, L.; Kaisermann, A.; Bachar, D.; Christen, R.; Terrat, S.; Mathieu, O.; Leveque, J.; Mougel, C.; Henault, C.; et al. Stimulation of Different Functional Groups of Bacteria by Various Plant Residues as a Driver of Soil Priming Effect. *Ecosystems* **2013**, *16*, 810–822. [[CrossRef](#)]
59. Song, A.; Zhang, J.; Xu, D.; Wang, E.; Bi, J.; Asante-Badu, B.; Njyenawe, M.C.; Sun, M.; Xue, P.; Wang, S.; et al. Keystone microbial taxa drive the accelerated decompositions of cellulose and lignin by long-term resource enrichments. *Sci. Total Environ.* **2022**, *842*, 156814. [[CrossRef](#)]
60. Voriskova, J.; Baldrian, P. Fungal community on decomposing leaf litter undergoes rapid successional changes. *ISME J.* **2013**, *7*, 477–486. [[CrossRef](#)]
61. Jin, X.; Wang, Z.; Wu, F.; Li, X.; Zhou, X. Litter Mixing Alters Microbial Decomposer Community to Accelerate Tomato Root Litter Decomposition. *Microbiol. Spectr.* **2022**, *10*, e0018622. [[CrossRef](#)] [[PubMed](#)]
62. Espana, M.; Rasche, F.; Kandeler, E.; Brune, T.; Rodriguez, B.; Bending, G.D.; Cadisch, G. Assessing the effect of organic residue quality on active decomposing fungi in a tropical Vertisol using N-15-DNA stable isotope probing. *Fungal Ecol.* **2011**, *4*, 115–119. [[CrossRef](#)]
63. Purahong, W.; Wubet, T.; Lentendu, G.; Schloter, M.; Pecyna, M.J.; Kapturska, D.; Hofrichter, M.; Krueger, D.; Buscot, F. Life in leaf litter: Novel insights into community dynamics of bacteria and fungi during litter decomposition. *Mol. Ecol.* **2016**, *25*, 4059–4074. [[CrossRef](#)] [[PubMed](#)]
64. Osono, T. Ecology of ligninolytic fungi associated with leaf litter decomposition. *Ecol. Res.* **2007**, *22*, 955–974. [[CrossRef](#)]
65. Cenini, V.L.; Fornara, D.A.; McMullan, G.; Ternan, N.; Carolan, R.; Crawley, M.J.; Clement, J.-C.; Lavorel, S. Linkages between extracellular enzyme activities and the carbon and nitrogen content of grassland soils. *Soil Biol. Biochem.* **2016**, *96*, 198–206. [[CrossRef](#)]
66. Wilhelm, R.C.; Cardenas, E.; Leung, H.; Szeitz, A.; Jensen, L.D.; Mohn, W.W. Long-Term Enrichment of Stress-Tolerant Cellulolytic Soil Populations following Timber Harvesting Evidenced by Multi-Omic Stable Isotope Probing. *Front. Microbiol.* **2017**, *8*, 537. [[CrossRef](#)] [[PubMed](#)]
67. Clocchiatti, A.; Hannula, S.E.; van den Berg, M.; Korthals, G.; de Boer, W. The hidden potential of saprotrophic fungi in arable soil: Patterns of short-term stimulation by organic amendments. *Appl. Soil Ecol.* **2020**, *147*, 103434. [[CrossRef](#)]
68. Miao, Y.; Lin, Y.; Chen, Z.; Zheng, H.; Niu, Y.; Kuzyakov, Y.; Liu, D.; Ding, W. Fungal key players of cellulose utilization: Microbial networks in aggregates of long-term fertilized soils disentangled using C-13-DNA-stable isotope probing. *Sci. Total Environ.* **2022**, *832*, 155051. [[CrossRef](#)] [[PubMed](#)]
69. Miao, Y.; Li, J.; Li, Y.; Niu, Y.; He, T.; Liu, D.; Ding, W. Long-Term Compost Amendment Spurs Cellulose Decomposition by Driving Shifts in Fungal Community Composition and Promoting Fungal Diversity and Phylogenetic Relatedness. *mBio* **2022**, *13*, e0032322. [[CrossRef](#)]
70. Koehler, C.; Campbell, A.N.; Pepe-Ranney, C.; Buckley, D.H. Assessing fungal contributions to cellulose degradation in soil by using high-throughput stable isotope probing. *Soil Biol. Biochem.* **2019**, *130*, 150–158. [[CrossRef](#)]
71. Rodrigues, P.d.O.; Alves Gurgel, L.V.; Pasquini, D.; Badotti, F.; Goes-Neto, A.; Baffi, M.A. Lignocellulose-degrading enzymes production by solid-state fermentation through fungal consortium among Ascomycetes and Basidiomycetes. *Renew. Energy* **2020**, *145*, 2683–2693. [[CrossRef](#)]
72. Liao, H.; Li, S.; Wei, Z.; Shen, Q.; Xu, Y. Insights into high-efficiency lignocellulolytic enzyme production by *Penicillium oxalicum* GZ-2 induced by a complex substrate. *Biotechnol. Biofuels* **2014**, *7*, 162. [[CrossRef](#)] [[PubMed](#)]
73. Oates, N.C.; Abood, A.; Schirmacher, A.M.; Alessi, A.M.; Bird, S.M.; Bennett, J.P.; Leadbeater, D.R.; Li, Y.; Dowle, A.A.; Liu, S.; et al. A multi-omics approach to lignocellulolytic enzyme discovery reveals a new ligninase activity from *Parascedosporium putredinis* NO1. *Proc. Natl. Acad. Sci. USA* **2021**, *118*, e2008888118. [[CrossRef](#)] [[PubMed](#)]
74. Cui, J.; Song, D.; Dai, X.; Xu, X.; He, P.; Wang, X.; Liang, G.; Zhou, W.; Zhu, P. Effects of long-term cropping regimes on SOC stability, soil microbial community and enzyme activities in the Mollisol region of Northeast China. *Appl. Soil Ecol.* **2021**, *164*, 103941. [[CrossRef](#)]

75. de Vries, F.T.; Manning, P.; Tallowin, J.R.B.; Mortimer, S.R.; Pilgrim, E.S.; Harrison, K.A.; Hobbs, P.J.; Quirk, H.; Shipley, B.; Cornelissen, J.H.C.; et al. Abiotic drivers and plant traits explain landscape-scale patterns in soil microbial communities. *Ecol. Lett.* **2012**, *15*, 1230–1239. [[CrossRef](#)] [[PubMed](#)]
76. Adetunji, A.T.; Lewu, F.B.; Mulidzi, R.; Ncube, B. The biological activities of beta-glucosidase, phosphatase and urease as soil quality indicators: A review. *J. Soil Sci. Plant Nutr.* **2017**, *17*, 794–807. [[CrossRef](#)]
77. Kellner, H.; Luis, P.; Pecyna, M.J.; Barbi, F.; Kapturska, D.; Krueger, D.; Zak, D.R.; Marmeisse, R.; Vandenbol, M.; Hofrichter, M. Widespread Occurrence of Expressed Fungal Secretory Peroxidases in Forest Soils. *PLoS ONE* **2014**, *9*, e95557. [[CrossRef](#)]

Disclaimer/Publisher’s Note: The statements, opinions and data contained in all publications are solely those of the individual author(s) and contributor(s) and not of MDPI and/or the editor(s). MDPI and/or the editor(s) disclaim responsibility for any injury to people or property resulting from any ideas, methods, instructions or products referred to in the content.